

# No Scratch Quantum Computing by Reducing Qubit Overhead for Efficient Arithmetics

Omid Faizy<sup>1,2,3,4</sup>, Norbert Wehn<sup>3</sup>, Paul Lukowicz<sup>4,5</sup>, and Maximilian Kiefer-Emmanouilidis<sup>4,5</sup>

<sup>1</sup> Laboratoire de Chimie de la Matière Condensée de Paris, UMR CNRS 7574, Sorbonne Université, 4, place Jussieu, 75252 Paris, France.

<sup>2</sup> Laboratoire de Mathématiques Pures et Appliquées Joseph Liouville, Université du Littoral Côte d’Opale, 50 rue Ferdinand Buisson, CS 80699, 62228 Calais, France.

<sup>3</sup> Microelectronic Systems Design (EMS), RPTU Kaiserslautern-Landau, Germany

<sup>4</sup> Department of Computer Science and Research Initiative QC-AI, RPTU Kaiserslautern-Landau, Kaiserslautern, Germany.

<sup>5</sup> German Research Center for Artificial Intelligence (DFKI), Kaiserslautern, Germany.

**Abstract.** Quantum arithmetic computation requires a substantial number of scratch qubits to stay reversible. These operations necessitate qubit and gate resources equivalent to those needed for the larger of the input or output registers due to state encoding. Quantum Hamiltonian Computing (QHC) introduces a novel approach by encoding input for logic operations within a single rotating quantum gate. This innovation reduces the required qubit register  $N$  to the size of the output states  $O$ , where  $N = \log_2 O$ . Leveraging QHC principles, we present reversible half-adder and full-adder circuits that compress the standard Toffoli + CNOT layout [Vedral et al., PRA, 54, 11, (1996)] from three-qubit and four-qubit formats for the Quantum half-adder circuit and five sequential Fredkin gates using five qubits [Moutinho et al., PRX Energy 2, 033002 (2023)] for full-adder circuit; into a two-qubit,  $4 \times 4$  Hilbert space. This scheme, presented here, is optimized for classical CMOS energy limitations to certain degree. Although we avoid superposition of input and output states in this manuscript, this remains feasible in principle. We see the best application for QHC in finding the minimal qubit and gate resources needed to evaluate any truth table, advancing FPGA capabilities using integrated quantum circuits or photonics.

**Keywords:** Quantum Arithmetics · Quantum Hamiltonian Computing · Adder.

## 1 Introduction

The question of minimal and most efficient arithmetic operators is approaching the atomic limits. Below a few hundred atoms per transistor, leakage and energy dissipation at least  $kT \ln 2$  per bit become prohibitive [1–3]. Reversible quantum logic can bypass these bounds to a certain degree [2–4]. Following this principle, early quantum adders [4, 5] implemented binary addition using Toffoli and CNOT gates, but at the expense of extra “scratch” qubits for reversibility and state embedding. For instance, standard reversible half-adder and full-adder circuits require three and four qubits, respectively, in order to produce sum and carry outputs without erasing the inputs. This “scratch” qubit overhead not only increases the Hilbert space (dimension 8 for three and dimension 16 for four qubits) but also adds numerous gates to uncompute intermediate results, complicating practical implementation. More recent designs reduce either the T-count or the ancilla count—sometimes to one or even zero [6–8], where additional ancillas refer to extra qubits beyond three qubits for half-adders and four qubits for full-adders.

Quantum Hamiltonian Computing (QHC) encodes Boolean inputs in Hamiltonian matrix elements rather than basis populations, minimizing the state count for logic gates [9–12]. Previous QHC studies implemented on single-molecule platforms realized 4-state half-adders and 8-state full-adders that required no qubits and relied on intrinsically irreversible dynamics; later work introduced multi-energy read-out schemes to compress the effective Hamiltonian even further [11, 12].

Theoretical studies show that classical data can be encoded as rotation angles in a QHC circuit by using a nano-graphene molecule doubly functionalized with nitro groups and bridged by graphene electrodes, whose nitro-group rotations serve as binary inputs that collectively implement a half-adder Boolean operation. [13].

Adapting these ideas to quantum computing is to find a unitary  $U(\boldsymbol{\theta}) = \exp(-iH(\boldsymbol{\theta})t)$  that depending on the binary inputs formulates the wanted logical output of any given truth table for the given input  $\boldsymbol{\theta}$ . From this point of view we argue that we can formulate a quantum representation (in the form of a quantum gate) which yields a given output (following the corresponding truth table) with only  $N = \log_2(O)$  where  $N$  is the number of qubits and  $O$  is the number of possible outputs.

Using the QHC paradigm, we present constructed reversible half- and full-adder circuits using only two qubits. This represents a significant reduction in the required resources compared to conventional designs. Both our half-adder and full-adder operate within a  $4 \times 4$  Hilbert-space (two qubits), rather than the  $8 \times 8$  (three qubit), or  $16 \times 16$  (four qubits) or larger spaces required by previous methods.

## 2 Circuit design

Starting with the half-adder as depicted in Fig. 1 (a), the device employs two qubits prepared in  $|\psi(t=0)\rangle = |00\rangle$ . A  $4 \times 4$  unitary  $\mathcal{U}(\alpha, \beta)$  confines dynamics to a protected sub-manifold and encodes the angles  $(\alpha, \beta) \in \{0, 1\}^2$  as logical inputs. The  $\mathcal{U}(\alpha, \beta)$  filters and maps resulting amplitudes onto the final qubits, which are then measured in the computational basis for SUM (XOR) and CARRY (AND) outputs.

$$\mathcal{U}(\alpha, \beta) = \begin{pmatrix} A & B - F & 0 & B + F \\ B + F & A & 0 & B - F \\ 0 & 0 & 1 & 0 \\ B - F & B + F & 0 & A \end{pmatrix}, \quad (1)$$

where

$$\begin{aligned} A &= \frac{1}{3} \left( 2 \cos \left( \frac{2}{3} \pi (\alpha + \beta) \right) + 1 \right), \\ B &= \frac{1}{3} \left( 1 - \cos \left( \frac{2}{3} \pi (\alpha + \beta) \right) \right), \\ F &= \frac{\sin \left( \frac{2}{3} \pi (\alpha + \beta) \right)}{\sqrt{3}}. \end{aligned} \quad (2)$$

Given the initial state  $|00\rangle = (1 \ 0 \ 0 \ 0)^T$  we can fulfill the half-adder truth table and response as:

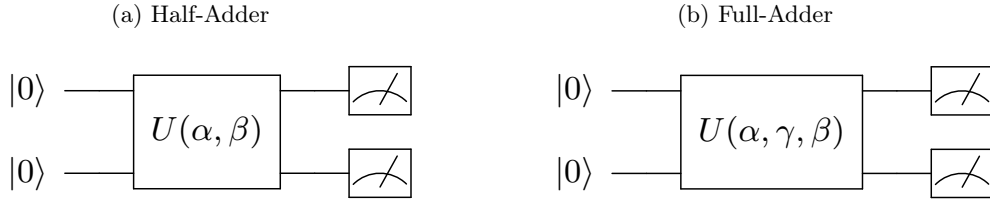


Fig. 1: (a) Two-Qubit QHC-Half-Adder circuit with classical binary inputs  $\alpha$  and  $\beta$  implemented directly inside circuit. (b) Two-Qubit QHC-Full-Adder circuit with classical binary inputs  $\alpha$ ,  $\gamma$  and  $\beta$  implemented directly inside circuit.

$$\begin{aligned}
 \mathcal{U}(0, 0) |00\rangle &= |00\rangle \\
 \mathcal{U}(0, 1) |00\rangle &= |01\rangle \\
 \mathcal{U}(1, 0) |00\rangle &= |01\rangle \\
 \mathcal{U}(1, 1) |00\rangle &= |11\rangle
 \end{aligned} \tag{3}$$

We can generalize now the protocol with full-adder as depicted in Fig. 1 (b). Again the device employs two qubits prepared in  $|\psi(t=0)\rangle = |00\rangle$ . A  $4 \times 4$  unitary  $\mathcal{U}(\alpha, \gamma, \beta)$  confines dynamics to a protected sub-manifold and encodes the angles  $(\alpha, \gamma, \beta) \in \{0, 1\}^2$  as logical inputs. The  $\mathcal{U}(\alpha, \gamma, \beta)$  filters and maps the resulting amplitudes to the final qubits, which are then measured in the computational basis for the SUM (XOR) and CARRY outputs.

The corresponding matrix has the following form:

$$\mathcal{U}(\alpha, \gamma, \beta) = \frac{1}{4} \begin{pmatrix} l+2m+1 & -2n-p-iq+1 & l-2m+1 & 2n-p-iq+1 \\ 2n-p-iq+1 & l+2m+1 & -2n-p-iq+1 & l-2m+1 \\ l-2m+1 & 2n-p-iq+1 & l+2m+1 & -2n-p-iq+1 \\ -2n-p-iq+1 & l-2m+1 & 2n-p-iq+1 & l+2m+1 \end{pmatrix}, \tag{4}$$

where

$$\begin{aligned}
 l &= e^{i\pi(\alpha+\beta+\gamma)}, \\
 m &= \cos\left(\frac{1}{2}\pi(\alpha+\beta+\gamma)\right), \\
 n &= \sin\left(\frac{1}{2}\pi(\alpha+\beta+\gamma)\right), \\
 p &= \cos(\pi(\alpha+\beta+\gamma)), \\
 q &= \sin(\pi(\alpha+\beta+\gamma)).
 \end{aligned} \tag{5}$$

See Sec. 4 Appendix for the corresponding steps to arrive at Eq. (4). Applying the full-adder gate we receive the corresponding truth table

$$\begin{aligned}
 \mathcal{U}(0, 0, 0) |00\rangle &= |00\rangle & \mathcal{U}(0, 0, 1) |00\rangle &= |01\rangle \\
 \mathcal{U}(0, 1, 0) |00\rangle &= |01\rangle & \mathcal{U}(0, 1, 1) |00\rangle &= |10\rangle \\
 \mathcal{U}(1, 0, 0) |00\rangle &= |01\rangle & \mathcal{U}(1, 0, 1) |00\rangle &= |10\rangle \\
 \mathcal{U}(1, 1, 0) |00\rangle &= |11\rangle & \mathcal{U}(1, 1, 1) |00\rangle &= |11\rangle.
 \end{aligned} \tag{6}$$

### 3 Conclusion

In this study, we presented Quantum Hamiltonian Computing as a method for performing quantum arithmetic operations, which reduces qubit overhead by encoding classical inputs within a single quantum gate. Our two-qubit half- and full-adder circuits in a  $4 \times 4$  Hilbert space require fewer resources than traditional textbook reversible design built from a Toffoli plus clean-up gates [4, 5, 14, 15]. Leveraging unitary evolution enables us to bypass classical CMOS energy limitations and achieve reversible logic with fewer qubits and gates, where the qubit count is only logarithmic in dependence on possible output states. Furthermore, the QHC unitary realizes the complete truth-table in one analogue pulse, as long as the gate can be implemented on the corresponding quantum hardware. While the current design targets classical logic without utilizing superposition of input and output states, it should be clear that this is possible in principle and can be as simple as converting the inputs from binary to real value inputs. However, the found unitaries are not fully expressive but can only map a sub-manifold in the Hilbert space. Removing this limitation, would lead again to scratch qubits thus no benefit to previous implementations [4]. However, the sub-manifold can be optimized to evaluate to superposition states expected to become most prominent in the circuit without the need to introduce qubits.

The QHC framework shows promise for advancement of FPGA designs by taking advantage of quantum architectures to minimize energy consumption. This approach offers potential applications in quantum circuits, integrated quantum photonics, and other emerging technologies, especially as the operational speeds of integrated quantum photonic devices, for example, can exceed those of classical computers [16].

### Acknowledgments

We would like to thank the Research Initiative ‘Quantum Computing for Artificial Intelligence’ (QC-AI) for their support.

### 4 Appendix: Full-adder unitary matrix $\mathcal{U}(\alpha, \gamma, \beta)$ construction

Let the computational basis of two qubits be ordered as  $\{|00\rangle, |01\rangle, |10\rangle, |11\rangle\}$ . We could fix the column vector (the *control* or *eigenvector*) as:

$$V = |00\rangle, \tag{A.1}$$

and three real parameters  $\alpha, \gamma, \beta \in \mathbb{R}$ . The task is to build a  $4 \times 4$  unitary matrix  $U(\alpha, \gamma, \beta)$  such that, when each parameter is restricted to the Boolean set  $\{0, 1\}$ , the eight input triples are mapped as

$$\begin{array}{c|c} (\alpha, \gamma, \beta) & U(\alpha, \gamma, \beta) V \\ \hline (0, 0, 0) & |00\rangle \\ (0, 0, 1) & |01\rangle \\ (0, 1, 0) & |01\rangle \\ (0, 1, 1) & |10\rangle \\ (1, 0, 0) & |01\rangle \\ (1, 0, 1) & |10\rangle \\ (1, 1, 0) & |10\rangle \\ (1, 1, 1) & |11\rangle \end{array}$$

We define now a 4-cycle permutation matrix  $\mathcal{R}$  as

$$\mathcal{R} = |01\rangle\langle 00| + |10\rangle\langle 01| + |11\rangle\langle 10| + |00\rangle\langle 11|. \quad (\text{A.2})$$

Equation (A.2) permutes the basis cyclically  $|00\rangle \rightarrow |01\rangle \rightarrow |10\rangle \rightarrow |11\rangle \rightarrow |00\rangle$ ; hence  $\mathcal{R}^4 = I_4$ . Written as a matrix,

$$\mathcal{R} = \begin{pmatrix} 0 & 0 & 0 & 1 \\ 1 & 0 & 0 & 0 \\ 0 & 1 & 0 & 0 \\ 0 & 0 & 1 & 0 \end{pmatrix}, \quad \mathcal{R}^\dagger \mathcal{R} = I_4.$$

Because  $\mathcal{R}$  is unitary, the principal matrix logarithm

$$\mathcal{R} = e^{-iH}, \quad H = i \log \mathcal{R}, \quad H^\dagger = H, \quad (\text{A.3})$$

is Hermitian. (The eigenvalues of  $\mathcal{R}$  are the fourth roots of unity  $\{1, i, -1, -i\}$ .) the three-parameter family could be Defined as

$$U(\alpha, \gamma, \beta) = \exp[-i(\alpha + \gamma + \beta)H] \quad (\text{A.4})$$

Some algebra leads to Eq. (4).

## References

1. R. Landauer, "Irreversibility and heat generation in the computing process," *IBM Journal of Research and Development*, vol. 5, no. 3, pp. 183–191, 1961.
2. C. H. Bennett, "Logical reversibility of computation," *IBM journal of Research and Development*, vol. 17, no. 6, pp. 525–532, 1973.
3. G. Chiribella, Y. Yang, and R. Renner, "Fundamental energy requirement of reversible quantum operations," *Phys. Rev. X*, vol. 11, p. 021014, Apr 2021.
4. V. Vedral, A. Barenco, and A. Ekert, "Quantum networks for elementary arithmetic operations," *Physical Review A*, vol. 54, no. 1, p. 147, 1996.
5. S. A. Cuccaro, T. G. Draper, S. A. Kutin, and D. P. Moulton, "A new quantum ripple-carry addition circuit," *arXiv preprint quant-ph/0410184*, 2004.
6. C. Gidney, "Halving the cost of quantum addition," *Quantum*, vol. 2, p. 74, 2018.
7. M. Remaud and V. Vandaele, "Ancilla-free quantum adder with sublinear depth," *arXiv:2501.16802*, 2025.
8. H. Nie, J. Khattar, and Y. Takahashi, "Optimising t- and cnot-gates in quantum ripple-carry adders," *arXiv:2401.17921*, 2024.
9. G. Dridi, R. Julien, M. Hliwa, and C. Joachim, "The mathematics of a quantum hamiltonian computing half adder boolean logic gate," *Nanotechnology*, vol. 26, p. 344003, aug 2015.
10. F. Ample, O. Faizy, H. Kawai, and C. Joachim, "The design of a surface atomic scale logic gate with molecular latch inputs," in *On-Surface Atomic Wires and Logic Gates* (M. Kolmer and C. Joachim, eds.), (Cham), pp. 139–155, Springer International Publishing, 2017.
11. G. Dridi, O. F. Namarvar, and C. Joachim, "Qubits and quantum hamiltonian computing performances for operating a digital boolean 1/2-adder," *Quantum Science and Technology*, vol. 3, no. 2, p. 025005, 2018.
12. O. F. Namarvar, O. Giraud, B. Georgeot, and C. Joachim, "Quantum hamiltonian computing protocols for molecular electronics boolean logic gates," *Quantum Science and Technology*, vol. 4, no. 3, p. 035009, 2019.
13. S. Srivastava, H. Kino, and C. Joachim, "Quantum half-adder boolean logic gate with a nanographene molecule and graphene nano-electrodes," *Chemical Physics Letters*, vol. 667, pp. 301–306, 2017.

14. M. Amy, D. Maslov, M. Mosca, and M. Roetteler, “A meet-in-the-middle algorithm for fast synthesis of depth-optimal quantum circuits,” *IEEE Transactions on Computer-Aided Design of Integrated Circuits and Systems*, vol. 32, no. 6, pp. 818–830, 2013.
15. P. Selinger, “Quantum circuits of  $t$ -depth one,” *Phys. Rev. A*, vol. 87, p. 042302, Apr 2013.
16. L. Labonté, O. Alibart, V. D’Auria, F. Doutre, J. Etesse, G. Sauder, A. Martin, E. Picholle, and S. Tanzilli, “Integrated photonics for quantum communications and metrology,” *PRX Quantum*, vol. 5, p. 010101, Feb 2024.